Electronic and optical properties of strained $In_xGa_{1-x}As/GaAs$ and strain-free $GaAs/Al_{0.3}Ga_{0.7}As$ quantum dots on (110) substrates

Ranber Singh* and Gabriel Bester†
Max-Planck-Institut für Festkörperforschung, Heisenbergstrasse 1, 70569 Stuttgart, Germany
(Received 12 July 2013; published 22 August 2013)

We investigate strained $In_xGa_{1-x}As/GaAs$ and strain-free $GaAs/Al_{0.3}Ga_{0.7}As$ quantum dots (QDs) grown on (110)-oriented substrates by means of atomic empirical pseudopotentials and configuration interaction. We find that there is a significant piezoelectric effect on the exciton fine structure splitting (FSS) in strained QDs due to the in-plane character of the electric field. The ground-state bright excitons in these QDs are polarized along the [001] and [$\bar{1}$10] crystal directions, and have large FSSs. The linear degree of polarization is large and decreases linearly with an increase in Ga content, while it is nearly zero and independent of Ga content in $In_xGa_{1-x}As/GaAs$ QDs with similar shape and size grown on (001) substrates.

DOI: 10.1103/PhysRevB.88.075430 PACS number(s): 73.21.Hb, 42.50.−p, 73.21.La, 78.67.Hc

I. INTRODUCTION

Semiconductor heterostructures grown on (110)-oriented substrates offer promising prospects for nonmagnetic spintronic devices.[1–5] In particular, quantum wells grown on (110)-oriented substrates are promising candidates for nonmagnetic spin transistors,[2] magnetic field sensors,[4] and spin resonant tunnel diodes.[5] There is a unique characteristic of spin-orbit pseudomagnetic field in the [110] direction in III-V semiconductors[6] leading to a relatively long electron spin lifetime, even at room temperature.[7] Long spin lifetime is an important property sought in semiconductor quantum dots (QDs) in order to use them in spintronics or quantum information processing.[8] Conventional self-assembled semiconductor QDs are, however, grown on (001)-oriented substrates, either by Stranski-Krastanov self-assembled growth,[9,10] leading to strained QDs such as $In_xGa_{1-x}As$ QDs embedded in GaAs. or by a modified droplet epitaxy method,[11] or by filling self-assembled nanoholes[12] leading to strain-free QDs, such as GaAs/AlGaAs. The growth of self-assembled QDs on (110)-oriented substrates is more challenging because layer-by-layer epitaxial growth is prevented by the formation of misfit dislocations.[13,14] However, QDs on (110)-oriented substrates can be grown on an ultrathin AlAs layer on a GaAs substrate[15] by using specific growth conditions and the cleaved-edge overgrowth technique.[16,17] Recently,[18] another molecular beam epitaxy technique has emerged enabling the growth of $In_xGa_{1-x}As/GaAs(110)$ QDs based on the modification of the incorporation kinetics of adatoms induced by the presence of chemisorbed atomic hydrogen. Strain-free GaAs/Al(Ga)As (110) QDs have been grown for a few years using droplet epitaxy.[19] Still, the growth of QDs on (110) surfaces is not fully understood and remains challenging.[20] The characterization of shape, size, and composition profile of these types of structure is far from the level of detail that has been reached in recent decades for (001)-grown QDs. However, the existence of a few QDs recently grown on (110) substrates allows us to speculate that the level of control will improve in the future, making these types of structure a realistic alternative with a possible long spin lifetime.

The electronic and optical properties of QDs grown on (001)- and (111)-oriented substrates have been extensively investigated both experimentally and theoretically. Based upon their unique optical properties these QDs have been proposed for various potential applications such as sources of *on-demand* triggered single photons, entangled photon pairs, quantum bits, etc. However, a detailed theoretical investigation of the electronic and optical properties of QDs grown on (110)-oriented substrates is still missing. It is not yet clear how far these types of QD differ from the ones grown on (001) and (111) substrates. In this paper, we investigate the electronic and optical properties of these QDs using the atomistic pseudopotential method[21,22] and the configuration-interaction approach.[23] We find that there is a significant piezoelectric effect on the electronic and optical properties of these QDs, in contrast to quantum wells that lack such a field. The bright-exciton states in these QDs are polarized along the [001] and [$\bar{1}$10] crystal directions, and show a large fine structure splitting (FSS) compared to the (001)-grown QDs.

II. COMPUTATIONAL DETAILS

We consider lens-shaped $In_xGa_{1-x}As/GaAs$ and $GaAs/Al_{0.3}Ga_{0.7}As$ QDs grown on (110)-oriented substrates with circular base (base diameter of 25.2 nm and height 3.5 nm). We construct the simulation cell by placing 3×10^6 atoms onto their unrelaxed zinc-blende atomic positions. The QD atoms are surrounded by the atoms constituting the barrier. This barrier has to be thick enough to allow for a full confinement of the QD wave functions, and in the strained QD case, for a decay of the QD-induced strain at the boundary. The position of all the atoms is relaxed to minimize the strain energy by the valence force field method.[24,25] The single-particle eigenfunctions and eigenenergies of the QDs are calculated by using the atomistic pseudopotential approach,[21,25] taking strain, band coupling, coupling between different parts of the Brillouin zone, and spin-orbit coupling into account. The atomistic description leads naturally to the correct symmetry and there is no need to adapt the basis set to the substrate orientation, as required in envelope function $\mathbf{k} \cdot \mathbf{p}$ approaches. The Coulomb and exchange integrals are calculated from the atomic wave functions as shown in Ref. 26 and the correlated excitonic states are calculated by the configuration-interaction (CI) approach.[23] For the CI calculations we use all possible determinants constructed

from the 12 lowest-energy electron and 12 highest hole states (spin included), thus accounting for correlations. We also investigate the effect of a piezoelectric field on the single-particle states and excitonic properties of strained $In_xGa_{1-x}As/GaAs$ (110) QDs.

III. RESULTS AND DISCUSSION

We investigate strained $In_xGa_{1-x}As/GaAs$ QDs with different compositions $x = 1,0.9,0.8,0.7,0.6$, and strain-free $GaAs/Al_{0.3}Ga_{0.7}As$ QDs. Figure 1 shows that in these QDs the $[\bar{1}10]$ and [001] crystal directions, which lie in the growth plane, are atomistically inequivalent and there is only one plane of reflection shown in Fig. 1(b) as a double-headed arrow. The corresponding atomistic symmetry of pure InAs or GaAs QDs on (110) substrates is C_S. Disk-shaped pure InAs or GaAs QDs on (110) surfaces have C_{2v} or C_S symmetry, depending on the local symmetry of the interfaces along the growth direction. However, in QDs grown on (001) substrates the atomistic symmetry for the pure InAs or GaAs QDs is C_{2v} and D_{2d} for lens- and disk-shaped QDs, respectively.[27] The alloy QDs belong formally only to the C_1 point group, with no symmetry operations.[28]

Strain and piezoelectricity are crucial in determining the properties of heterostructures[29,30] and self-assembled QDs.[31–36] The $GaAs/Al_{0.3}Ga_{0.7}As$ heterostructures are free of strain and hence of piezoelectric effects. However, strained $In_xGa_{1-x}As/GaAs$ heterostructures develop significant piezoelectric fields that strongly depend on the growth direction. When a strained-layer heterostructure is grown on certain crystallographic surfaces, such as $In_xGa_{1-x}As/GaAs$, the lattice-mismatch-induced strain generates a piezoelectric polarization given as a function of mechanical strain η_j in Voigt notation, retaining the second order in strain, as[33,36]

$$P_\mu = \sum_{j=1}^{6} e_{\mu j}\eta_j + \frac{1}{2}\sum_{jk=1}^{6} B_{\mu jk}\eta_j\eta_k, \qquad (1)$$

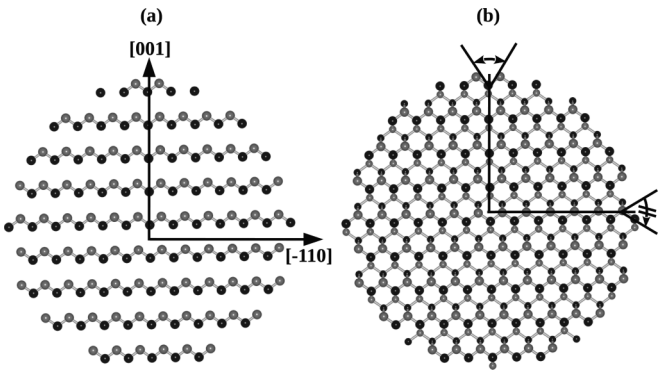

FIG. 1. (a) One monolayer (ML) and (b) two MLs in the (110) plane cut through the center of a QD grown on a (110) surface. The black (gray) spheres represent the cations (anions). The small spheres in (b) represent the corresponding cations (anions) in the atomic layer beneath (a). Atomistically the $[\bar{1}10]$ and [001] crystal directions, which lie in the growth plane, are inequivalent and only the $(\bar{1}10)$ plane is a reflection plane. The atomistic symmetry of pure InAs or GaAs lens-shaped QDs on (110) substrates is C_S. For alloyed QDs the symmetry is reduced to C_1.

where $e_{\mu j}$ is the proper piezoelectric tensor of the unstrained material and $B_{\mu jk}$ represents the first-order change of the piezoelectric tensor with strain.[36] Tabulated values of $e_{\mu j}$ and $B_{\mu jk}$ based on density functional theory have been presented in Ref. 36 and are used in this work.

For strained-layer superlattices grown along the [001] direction, the off-diagonal strain components are zero and no polarization fields are induced.[36] For structures grown along the [111] direction, all three off-diagonal strain components are equal and the resulting strain-induced polarization is directed along the [111] crystallographic growth direction. For strained-layer superlattices grown along the [110] direction the polarization is nearly as large as in the case of [111] growth and points along the [001] direction and therefore lies in the (110) growth plane. In such a superlattice or quantum well geometry, no piezoelectric field can form, however, for electrostatic reasons.[36]

In the case of QDs, the strain profile is more complex than in two-dimensional heterostructures. A QD grown on the (001) surface has significant strain along the [110] and $[1\bar{1}0]$ crystal directions due to the curved upper interface.[32] This strain gives rise to a rather small piezoelectric polarization.[33] In the case of QDs grown along the [111] direction the piezoelectric field is quite strong[27] and mainly oriented along the growth direction. However, this is the direction of strong confinement where the field has only a moderate effect on the shape of the wave functions. The optical properties are therefore only marginally affected.[27] In the case of QDs grown along the [110] direction, the polarization field lies in the growth plane and a piezoelectric field can develop; in contrast to the case of quantum wells where the periodicity of the structure in plane forbids such a field.[36] It can be expected that this field will be crucial for a correct description of these types of QD since the field will tend to pull electron and hole wave functions apart in the direction of weak confinement. Figure 2 shows the piezoelectric potential calculated according to Ref. 33 in $In_xGa_{1-x}As/GaAs$ QDs for $x = 1.0,0.8,0.6$. The piezoelectric field is mainly oriented along the [001] crystallographic direction, as expected. The polarization field reflects the atomistic crystal symmetry and shows one plane of reflection. The piezoelectric field in pure InAs QDs is very strong and decreases with an increase in the Ga content.

We now calculate the single-particle electron and hole states with and without piezoelectric field in strained and strain-free QDs. The squares of the wave functions for electrons (e_0,e_1,e_2) and holes (h_0,h_1,h_2) are given in Fig. 3, showing that in pure InAs QDs, without the piezoelectric effect, the e_1 and e_2 states are oriented along the $[\bar{1}10]$ and [001] crystallographic directions, respectively. As the Ga content is increased the e_1 (e_2) state rotates from $[\bar{1}10]$ ([001]) towards [001] ($[\bar{1}10]$). The hole states have an intricate probability distribution that originates from their multiband character. In pure InAs QDs, without the piezoelectric effect, the hole states have accumulations of probability distribution along the $[\bar{1}10]$ direction. In alloyed QDs the probability distribution of hole states is qualitatively similar to the one observed in conventional QDs grown along [001].[26] The inclusion of the piezoelectric field in $In_xGa_{1-x}As/GaAs$ QDs has no significant effect on the probability distribution of electron states except for a minute change in the orientation of the e_1 and e_2 states.

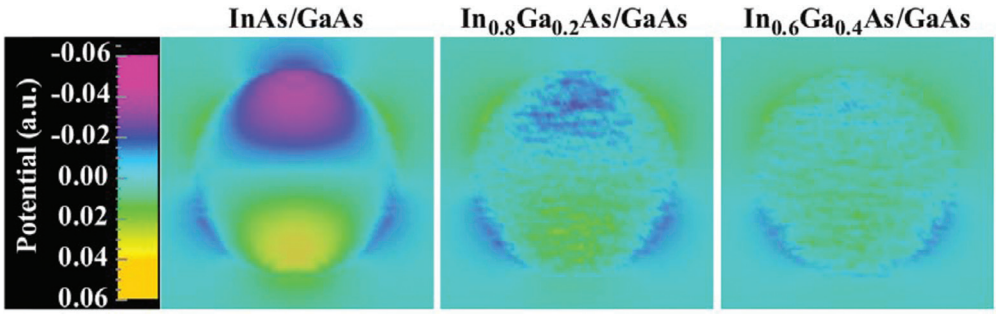

FIG. 2. (Color online) Piezoelectric potential in atomic units (a.u.) in $In_xGa_{1-x}As/GaAs$ QDs. In pure InAs QDs the piezoelectric field is quite strong and directed along the [001] crystallographic direction. The strength of this field decreases with an increase in the Ga content (decrease in strain).

However, the probability distribution of hole states changes to some extent, introducing a noticeable distortion along the [001] direction.

We further investigate the orbital and Bloch function characters of electron and hole single-particle states. As a consequence of the low atomistic symmetry of these QDs the electron and hole states are expected to have mixed orbital and Bloch function characters. In both C_1 and C_s symmetry the heavy-hole (HH) and light-hole (LH) states belong to the same irreducible representation, which allows effective mixing of these states. In the case of QDs grown on (001) surfaces the heavy- and light-hole states are energetically split by confinement and by biaxial strain. Consequently, the hole states have dominantly HH character.[26] However, in the case of QDs grown on the (110) surface, the confinement is along the [110] crystallographic direction and affects both the HH and LH states and does not lead to the clear energetic splitting of both states, as in [001] confinement. In these QDs the hole

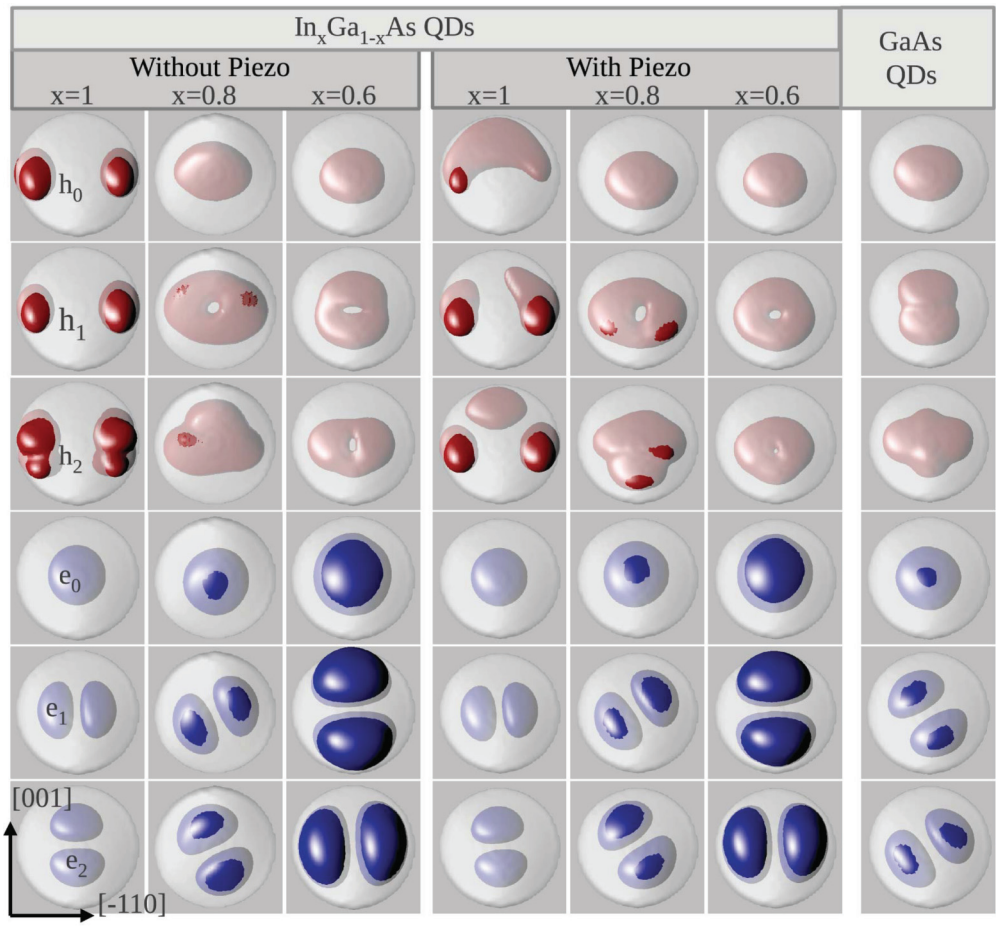

FIG. 3. (Color online) Single-particle wave functions squared, for electron (e_0, e_1, e_2) and hole (h_0, h_1, h_2) states in strained $In_xGa_{1-x}As/GaAs$ and strain-free $GaAs/Al_{0.3}Ga_{0.7}As$ QDs. The red and blue color isosurfaces correspond to 75% probability density for the hole and electron states, respectively. The white circular boundaries represent the physical dimensions of the QDs.

TABLE I. Decomposition of the wave functions of the highest three hole states (h_0,h_1,h_2) into the bulk Γ-point Bloch functions: heavy-hole (HH), light-hole (LH), split-off (SO), and conduction bands (el).

QD	State	HH	LH	SO	el
InAs	h_0	29.1	29.2	38.7	0.5
	h_1	26.2	33.2	37.2	0.6
	h_2	25.8	33.9	37.2	0.6
$In_{0.6}Ga_{0.4}As$	h_0	33.3	18.2	45.7	0.4
	h_1	31.3	21.7	44.1	0.4
	h_2	31.1	24.5	41.4	0.4
GaAs	h_0	29.2	52.1	17.7	0.2
	h_1	23.6	48.9	26.3	0.2
	h_2	27.2	45.1	26.5	0.3

states are expected to be highly mixed. This is precisely the case in our calculations, shown in Table I where we have projected the QD single-particle wave functions onto the three valence bands and the lowest conduction band of the bulk material at the Γ point. Table I shows that the hole states have a fully mixed Bloch function character.

Next, we plot in Fig. 4 the single-particle energies for the first six electron states $e_{0,1,\ldots,5}$ and first six hole states $h_{0,1,\ldots,5}$ with respect to the energy of e_0 for the electron states and of h_0 for the hole states. The connection to the GaAs QD is given as dashed lines, since the barrier material is changing from GaAs for $In_xGa_{1-x}As$ QDs to $Al_{0.3}Ga_{0.7}As$ for the GaAs QD, making these two system difficult to compare. With increasing In content, the confinement (the depth of the potential barrier) increases and the splitting between the states tends to increase

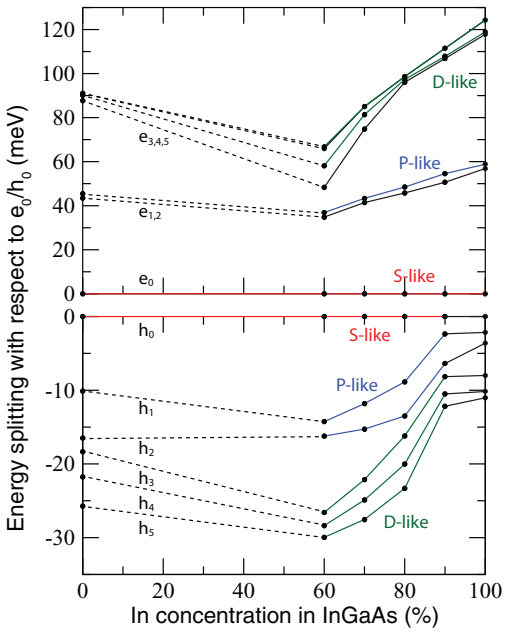

FIG. 4. (Color online) Single-particle energies for the first six electron $e_{0,1,\ldots,5}$ (upper panel) and first six hole $h_{0,1,\ldots,5}$ (lower panel) states with respect to the energy of e_0 for the electron states and of h_0 for the hole states. The connection to the pure GaAs QD is shown as dashed lines, as the barrier material is different than for the remaining data points.

for the electrons (top panel). The "shell structure" with equidistant *S*, *P*, and *D* states with degeneracies of 1, 2, and 3, well known for structures grown along the [001] direction, is recognizable for electronic states in [110]-grown structures for high In concentration. However, for low In concentrations, the splitting between the *P*-like and the *D*-like states decreases significantly. In the case of the hole states (lower panel), the situation is more complex because of the multiband character of the hole states in these QDs (see Table I). The *S*-, *P*-, and *D*-like states have different slopes as a function of In concentration and tend to merge for the pure InAs case. At this concentration, the ground-state hole h_0 has dominant *P* character (see Fig. 3).

The oscillator strengths for the excitonic transitions in $In_xGa_{1-x}As$ QDs including piezoelectricity are given in Figs. 5(a)–5(c). In Fig. 5(a) the oscillator strength has been multiplied by a factor of 4. The labels *SS*, *SP*, *PS*, *PP*, and *DD* must be interpreted with care, since the states have a significant degree of orbital character mixing. This mixing results in a significant oscillator strength from cross transitions, such as *SP*, which are much darker in [001]-grown structures. This feature represents a marked contrast between the [110] and [001] QD systems.

In Fig. 5(c) we plot the degree of linear polarization (DLP) defined as $\frac{I_{[110]}-I_{[1\bar{1}0]}}{I_{[110]}+I_{[1\bar{1}0]}}$ for conventional QDs (001) and $\frac{I_{[001]}-I_{[\bar{1}10]}}{I_{[001]}+I_{[\bar{1}10]}}$ for QDs grown on (110). This definition corresponds

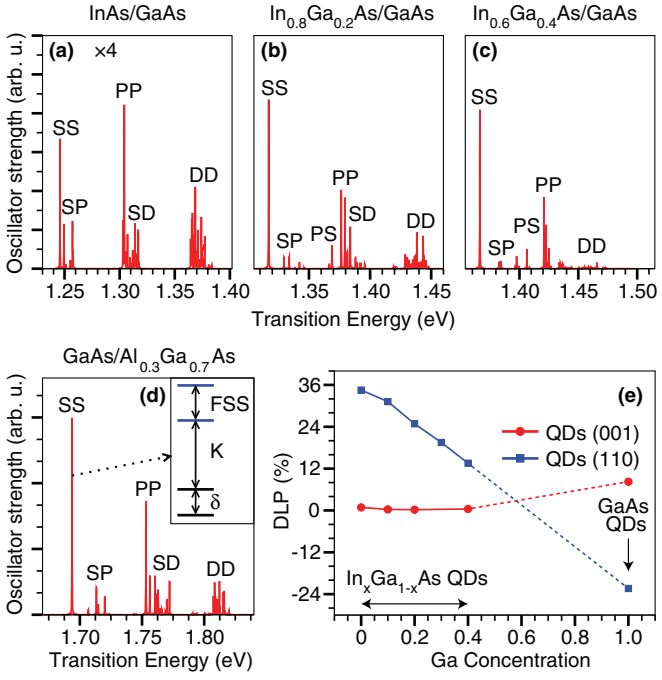

FIG. 5. (Color online) Oscillator strength of $In_xGa_{1-x}As$ QDs including the piezoelectricity effect (a)–(c) and in GaAs QDs (d). In (a) the oscillator strength has been multiplied by a factor of 4. The main dominant exciton transitions have been labeled as *SS*, SP, *PS*, *PP*, and *DD*, indicating the transitions from e_0 to h_0, e_0 to $h_{1,2}$, $e_{1,2}$ to $h_{1,2}$, etc. The inset in (d) represents schematically the fine structure of the ground-state (*SS*) transitions. The values of FSS, *K*, and δ in different QDs are given in Table II. The DLP (%) as a function of Ga content in QDs on (001) and (110) surfaces is given in (e).

TABLE II. Emission energy of lower bright exciton, FSS, dark-exciton doublet splitting (δ) and the splitting (K) between the lower bright exciton and the higher dark exciton in strained $In_xGa_{1-x}As/GaAs$ and strain-free $GaAs/Al_{0.3}Ga_{0.7}As$ QDs grown on the (110) surface.

QD material	Emission energy (eV)	FSS (μeV)	δ (μeV)	K (μeV)
	Neglecting piezoelectricity			
InAs	1.247	12.7	1.3	0.5
$In_{0.9}Ga_{0.1}As$	1.293	54.3	3.1	58.2
$In_{0.8}Ga_{0.2}As$	1.324	56.0	1.6	88.5
$In_{0.7}Ga_{0.3}As$	1.345	42.5	0.9	88.5
$In_{0.6}Ga_{0.4}As$	1.370	23.6	0.3	72.4
GaAs	1.694	48.3	7.4	92.2
	Including piezoelectricity			
InAs	1.246	18.2	3.4	16.5
$In_{0.9}Ga_{0.1}As$	1.290	73.8	8.1	52.6
$In_{0.8}Ga_{0.2}As$	1.317	73.8	4.7	74.9
$In_{0.7}Ga_{0.3}As$	1.342	54.2	2.4	77.4
$In_{0.6}Ga_{0.4}As$	1.366	30.7	0.8	65.9

to the DLP experimentally measured in emission at high temperatures. The DLP is very large in QDs grown on (110) and decreases linearly with an increase in Ga content.

The inset in Fig. 5(d) indicates schematically the fine structure of the ground-state exciton (SS) transitions. Due to the large HH-LH mixing in the (110) structures, the lowest two states are not completely dark but retain an oscillator strength approximately 800 times smaller than the oscillator strength we obtain for the bright states, for the $In_{0.6}Ga_{0.4}As$ QD. The values of FSSs, splitting from the lower bright exciton to the higher dark exciton (K), and the dark-exciton splitting (δ) in different QDs are given in Table II. Our emission energies are in good agreement with the experimental values for $In_xGa_{1-x}As$ QDs,[16–18,37] and for GaAs QDs.[19] These experiments have not delivered values for the FSS yet, but the observed exciton emission lines have large linewidths, which could indicate large FSSs. We obtain large FSSs and comparatively large dark-state splittings δ. The inclusion of piezoelectric fields has only a marginal effect on the emission energy but a significant effect on the FSS, δ, and K. The values of FSS, δ, and K are very unusual for pure InAs QDs, due to the P-type character of the highest-energy hole state h_0.

In summary, we studied the electronic and optical properties of $In_xGa_{1-x}As/GaAs$ and $GaAs/Al_{0.3}Ga_{0.7}As$ QDs grown on (110) substrates. There is a significant piezoelectric effect on the electronic and optical properties of $In_xGa_{1-x}As/GaAs$ QDs grown on (110)-oriented substrates. The hole states have highly mixed orbital and Bloch function characters. The inclusion of the piezoelectric field significantly changes the probability distribution of the hole states. The ground-state bright excitons are polarized along the [001] and [$\bar{1}$10] directions, and have a large fine structure splitting. The degree of linear polarization is large and decreases linearly with an increase in Ga content in $In_xGa_{1-x}As/GaAs$ QDs on a (110) substrate, while it is nearly zero and independent of Ga content in QDs of similar shape and size on (001) substrates. In strain-free $GaAs/Al_{0.3}Ga_{0.7}As$ QDs the DLP is large on both (001) and (110) substrates.

*Present address: Institute of Physical Chemistry and Center for Computational Sciences, Johannes Gutenberg University Mainz, Staudingerweg 9, D-55128 Mainz, Germany; singh@uni-mainz.de
†g.bester@fkf.mpg.de

[1] Y. Ohno, D. K. Young, B. Beschoten, F. Matsukura, H. Ohno, and D. D. Awschalom, Nature (London) **402**, 790 (1999).
[2] K. C. Hall, W. H. Lau, K. Gündoğdu, M. E. Flatté, and T. F. Boggess, Appl. Phys. Lett. **83**, 2937 (2003).
[3] J. Wunderlich, B. Kaestner, J. Sinova, and T. Jungwirth, Phys. Rev. Lett. **94**, 047204 (2005).
[4] K. C. Hall, K. Gündoğdu, J. L. Hicks, A. N. Kocbay, M. E. Flatté, T. F. Boggess, K. Holabird, A. Hunter, D. H. Chow, and J. J. Zinck, Appl. Phys. Lett. **86**, 202114 (2005).
[5] V. Sih, R. C. Myers, Y. K. Kato, W. H. Lau, A. C. Gossard, and D. D. Awschalom, Nat. Phys. **1**, 31 (2005).
[6] R. Eppenga and M. F. H. Schuurmans, Phys. Rev. B **37**, 10923 (1988).
[7] Y. Ohno, R. Terauchi, T. Adachi, F. Matsukura, and H. Ohno, Phys. Rev. Lett. **83**, 4196 (1999).
[8] A. Imamoglu, D. D. Awschalom, G. Burkard, D. P. DiVincenzo, D. Loss, M. Sherwin, and A. Small, Phys. Rev. Lett. **83**, 4204 (1999).
[9] N. Liu, J. Tersoff, O. Baklenov, A. L. Holmes, and C. K. Shih, Phys. Rev. Lett. **84**, 334 (2000).
[10] T. Walther, A. G. Cullis, D. J. Norris, and M. Hopkinson, Phys. Rev. Lett. **86**, 2381 (2001).
[11] K. Watanabe, N. Koguchi, and Y. Gotoh, Jpn. J. Appl. Phys. **39**, L79 (2000).
[12] A. Rastelli, S. M. Ulrich, E. M. Pavelescu, T. Leinonen, M. Pessa, P. Michler, and O. G. Schmidt, Superlattices Microstruct. **36**, 181 (2004).
[13] B. A. Joyce, T. S. Jones, and J. G. Belk, J. Vac. Sci. Technol. B **16**, 2373 (1998).
[14] J. G. Belk, D. W. Pashley, C. F. McConville, B. A. Joyce, and T. S. Jones, Surf. Sci. **410**, 82 (1998).
[15] D. Wasserman, S. A. Lyon, M. Hadjipanayi, A. Maciel, and J. F. Ryan, Appl. Phys. Lett. **83**, 5050 (2003).
[16] J. Bauer, D. Schuh, E. Uccelli, R. Schulz, A. Kress, F. Hofbauer, J. J. Finley, and G. Abstreiter, Appl. Phys. Lett. **85**, 4750 (2004).
[17] M. Blumin, H. E. Ruda, I. G. Savelyev, A. Shik, and H. Wang, J. Appl. Phys. **99**, 093518 (2006).
[18] L. Díez-Merino and P. Tejedor, J. Appl. Phys. **110**, 013106 (2011).
[19] T. Mano, T. Kuroda, T. Noda, and K. Sakoda, Phys. Status Solidi B **246**, 729 (2009).
[20] E. Uccelli, S. Nrnberger, M. Bichler, G. Abstreiter, and A. F. i Morral, Superlattices Microstruct. **44**, 425 (2008).
[21] L.-W. Wang and A. Zunger, Phys. Rev. B **59**, 15806 (1999).
[22] G. Bester, J. Phys.: Condens. Matter **21**, 023202 (2009).
[23] A. Franceschetti, H. Fu, L.-W. Wang, and A. Zunger, Phys. Rev. B **60**, 1819 (1999).
[24] P. N. Keating, Phys. Rev **145**, 637 (1966).

[25] A. J. Williamson, L.-W. Wang, and A. Zunger, Phys. Rev. B **62**, 12963 (2000).
[26] G. Bester, S. Nair, and A. Zunger, Phys. Rev. B **67**, 161306 (2003).
[27] R. Singh and G. Bester, Phys. Rev. Lett. **103**, 063601 (2009).
[28] R. Singh and G. Bester, Phys. Rev. Lett. **104**, 196803 (2010).
[29] E. A. Caridi, Ph.D. thesis, Cornell University, 1990.
[30] R. M. Martin, Phys. Rev. B **5**, 1607 (1972).
[31] F. Widmann, J. Simon, B. Daudin, G. Feuillet, J. L. Rouvière, N. T. Pelekanos, and G. Fishman, Phys. Rev. B **58**, R15989 (1998).
[32] G. Bester and A. Zunger, Phys. Rev. B **71**, 045318 (2005).
[33] G. Bester, A. Zunger, X. Wu, and D. Vanderbilt, Phys. Rev. B **74**, 081305 (2006).
[34] A. Schliwa, M. Winkelnkemper, and D. Bimberg, Phys. Rev. B **76**, 205324 (2007).
[35] S.-H. Park and Y.-H. Cho, J. Appl. Phys. **109**, 113103 (2011).
[36] A. Beya-Wakata, P.-Y. Prodhomme, and G. Bester, Phys. Rev. B **84**, 195207 (2011).
[37] M. Hadjipanayi, A. C. Maciel, J. F. Ryan, D. Wasserman, and S. A. Lyon, Appl. Phys. Lett. **85**, 2535 (2004).